

**Supporting Information for “Analytic gradient for the QM/MM-Ewald method using charges derived from the electrostatic potential: Theory, implementation, and application to *ab initio* molecular dynamics simulation of the aqueous electron”**

Zachary C. Holden, Bhaskar Rana, and John M. Herbert\*

*Department of Chemistry and Biochemistry,*

*The Ohio State University, Columbus, Ohio 43210 USA*

(Dated: March 3, 2019)

Here, we report results from some alternative simulations that are intended to help understand the nature of the energy fluctuations depicted in Fig. 4. Some of these are simulations of  $e^-(\text{aq})$  and others are simulations of neat liquid water, but in each case the simulation conditions are the same: a periodic simulation cell with  $L = 31.3192 \text{ \AA}$  containing 1,024 total water molecules (corresponding to normal liquid density), with 24 of those water molecules contained in the QM region. Initial velocities selected from a Maxwell-Boltzmann distribution at  $T = 300 \text{ K}$ . Except where otherwise specified, all simulations use a time step of  $\Delta t = 42 \text{ a.u.}$

Due to the highly contentious nature of the debate surrounding the structure of  $e^-(\text{aq})$ ,<sup>1-4</sup> we thought it best to begin our trajectories directly from snapshots taken from Ref. 5, in order to demonstrate that a cavity structure is preserved despite the abrupt change in the the level of theory. We note from Fig. 4 that the initial energy fluctuations are quite large, on the order of  $\pm 0.1 E_h$ . The magnitude of these fluctuations is an artifact (or consequence) of the system re-adjusting to a different water force field. Operationally, our simulations begin on a high-energy, repulsive portion of the potential surface, for no reason other than the fact that the water model is different in our work as compared to that used in Ref. 5, and large energy fluctuations result as the simulation equilibrates with respect to the change in the equilibrium geometry of  $\text{H}_2\text{O}$ . This can be verified by taking the structure from which the simulation in Fig. 4 was initiated and subjecting it to a few cycles of geometry optimization. In doing so, the energy very rapidly decreases by  $\approx 5,500 \text{ kcal/mol}$  or  $\approx 8.8 E_h$ , mostly associated with the bond-stretching terms in the water force field. An MD trajectory initialized at  $T = 300 \text{ K}$  from this partially-optimized structure exhibits dramatically smaller energy fluctuations. Figure S1 shows a close-up view of the first 1.0 ps of the simulation, starting from either the relaxed or the unrelaxed structure extracted

---

\* herbert@chemistry.ohio-state.edu

from the simulation in Ref. 5. (This represents the first 1.0 ps of the data plotted in Fig. 4.) The simulation that begins from the relaxed geometry exhibits much smaller energy fluctuations and no drift in the energy of 5.0 ps.

In view of this, one could reasonably argue that we ought to have derived our analysis from this pre-optimized trajectory, thus avoiding the large energy fluctuations. It is worth noting that our main conclusions are not affected by this choice, as demonstrated by the radial distribution functions (RDFs) that are plotted in Fig. S2. There, we compare the results presented in Fig. 8, which were obtained from the 5 ps trajectory without any initial relaxation, to those obtained from 1 ps of dynamics starting from the relaxed structure. Qualitatively, the results are extremely similar, with local maxima in  $g(r)$  that are found at precisely the same values of  $r$  in either case. What changes is that the peaks are narrower, and thus the cavity structure more well-defined, in the trajectory that starts from a relaxed geometry. In particular,  $g(r)$  goes all the way to zero in between its first and second maxima in this case. Presumably, this short trajectory starting from a relaxed geometry still needs to warm up a bit, at which point some of this sharpness would wash out. Clearly, however, a well-defined cavity is obtained in either case, with hydrogen and oxygen atoms completely excluded below some minimum distance.

Returning to the issue of energy fluctuations, an alternative way of looking at these results is that a smaller time step is required when using the unoptimized trajectory, since the early-time velocities are likely quite large as the simulation adjusts to the new water model. Figure S3 compares energy fluctuations from two different simulations starting from an unoptimized geometry, one with a time step of  $\Delta t = 42$  a.u. (as used for the simulations that we have analyzed in detail) and the other using a time step of  $\Delta t = 21$  a.u. (Although  $\Delta t = 42$  a.u.  $\approx 1.0$  fs is quite standard in classical MD, at least when all bonds are flexible, a time step of 0.5 fs is more typical in *ab initio* MD.<sup>6-8</sup>) Although no geometry optimization was performed prior to the simulations shown in Fig. S3, which should therefore experience very large initial velocities during the equilibration phase, the smaller time step is able to accommodate and affords energy fluctuations on par with those observed in Fig. S1 *after* geometry optimization.

Note also from Fig. S4 that the choice of an atom-centered Lebedev grid versus a uniform Cartesian grid (for evaluation of the electrostatic potential and subsequent fitting of CHELPG charges) makes absolute no difference in the overall energy fluctuations. This is despite the fact that the charges obtained are slightly different (at the level of  $\sim 10^{-2}$  a.u.) between the two grids, and that the total electronic energies differ by  $\sim 10^{-4} E_h$  depending on the choice of grid. The energy gradients are different as well, but clearly this effect is tiny in comparison to the magnitudes

of the total atomic gradients that are drive the molecular dynamics.

In order to investigate possible adverse consequences associated with use of Ewald summation for a unit cell with net charge, we extracted snapshots (at  $t_0 = 0$ , 2.5 ps, and 5.0 ps) from the simulation whose fluctuations are shown in Fig. 4, then continued the simulation from these snapshots but run as *neutral* liquid water. (This means that the neutral liquid water structure initially contains an empty solvent void where the electron used to be. Furthermore, to reduce the cost the basis set was changed from 3-21++G\* to 3-21G\*, since the diffuse basis functions should no longer be necessary.) Energy fluctuations from these simulations are shown in Fig. S5. For  $t_0 = 0$ , which corresponds to the same starting structure as in Fig. 4, we observe that the initial energy fluctuations are just as large as for the corresponding  $e^-(aq)$  simulation in Fig. 4, however these fluctuations are dramatically reduced for the  $t_0 = 2.5$  ps and  $t_0 = 5.0$  ps structures. This convincingly demonstrates that the large energy fluctuations observed in Fig. 4 have nothing to do with the hydrated electron *per se*, but rather originate in equilibration of the water force field. This equilibration is essentially complete by  $t = 2.5$  ps in Fig. 4, so that when this (and the subsequent  $t_0 = 5.0$  ps) snapshot is selected, initial energy fluctuations for the neutral water simulation are small.

Similarly, Fig. S6 shows a  $t_0 = 0$  simulation on neutral water that is carried out using the QM/MM-Ewald procedure but with Mulliken rather than CHELPG image charges. Initially energy fluctuations are essentially the same as those observed in Fig. 4, meaning that we should not ascribe these to the (much more complicated) CHELPG charge gradients either. In conclusion, all signals point to these fluctuations being nothing more than the normal equilibration upon switching the level of theory with respect to that used to generate the starting structures.

---

<sup>1</sup> L. Turi and A. Madarász, *Science* **331**, 1387 (2011).

<sup>2</sup> L. D. Jacobson and J. M. Herbert, *Science* **331**, 1387 (2011).

<sup>3</sup> R. E. Larsen, W. J. Glover, and B. J. Schwartz, *Science* **331**, 1387 (2011).

<sup>4</sup> J. M. Herbert and L. D. Jacobson, *J. Phys. Chem. A* **115**, 14470 (2011).

<sup>5</sup> F. Uhlig, O. Marsalek, and P. Jungwirth, *J. Phys. Chem. Lett.* **3**, 3071 (2012), erratum: *ibid.* **4**, 603 (2013).

<sup>6</sup> D. Marx and J. Hutter, *Ab Initio Molecular Dynamics: Basic Theory and Advanced Methods* (Cambridge University Press, Cambridge, United Kingdom, 2009).

<sup>7</sup> R. P. Steele, *J. Phys. Chem. A* **119**, 12119 (2015).

<sup>8</sup> J. D. Herr and R. P. Steele, *Chem. Phys. Lett.* **661**, 42 (2016).

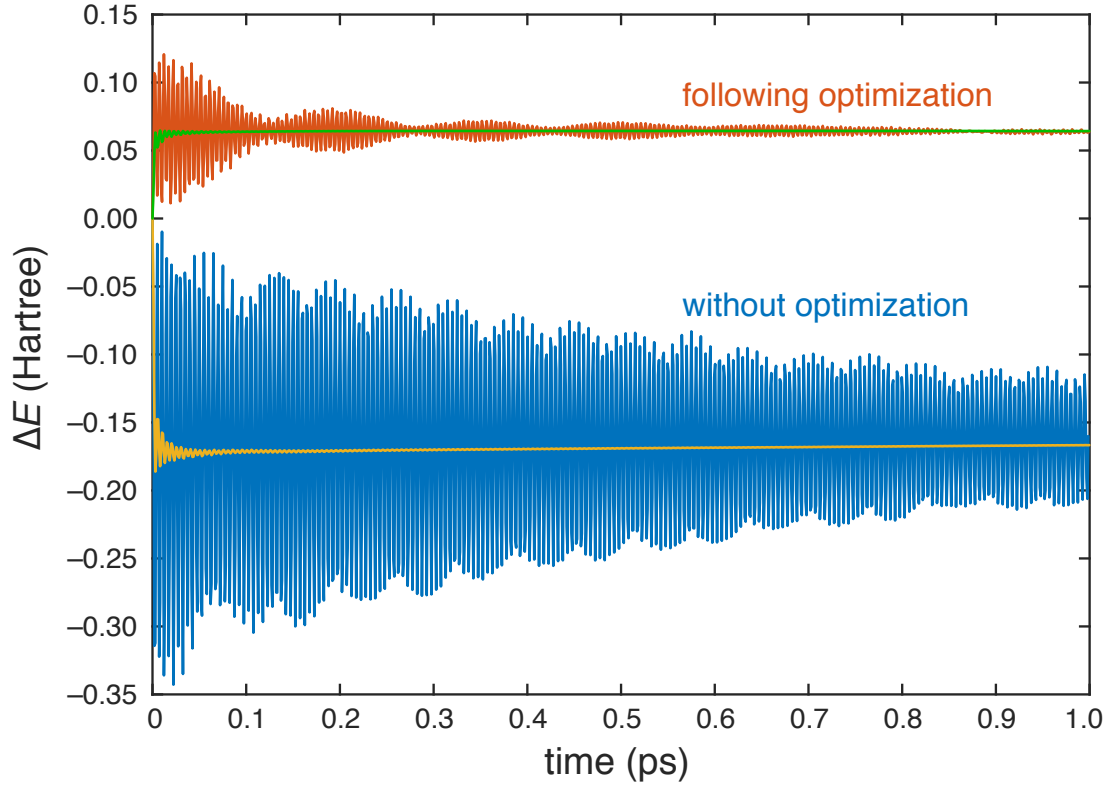


FIG. S1: Close-up view (representing the first 1.0 ps of the plot in Fig. 4) of the energy fluctuations in HF+D3/3-21++G\* simulations of  $e^-(aq)$ , starting either from the unoptimized structure whose geometry is taken directly from Ref. 5, or else from a structure that has been partially optimized at the QM/MM level of theory prior to the MD simulation, with HF+D3/3-21++G\* as the QM level. In the latter case, 128 geometry optimization steps were performed, during which the energy decreases by  $\approx 8.8 E_h$ . Nearly all of that energy lowering comes from the bond-stretching terms in the water force field.

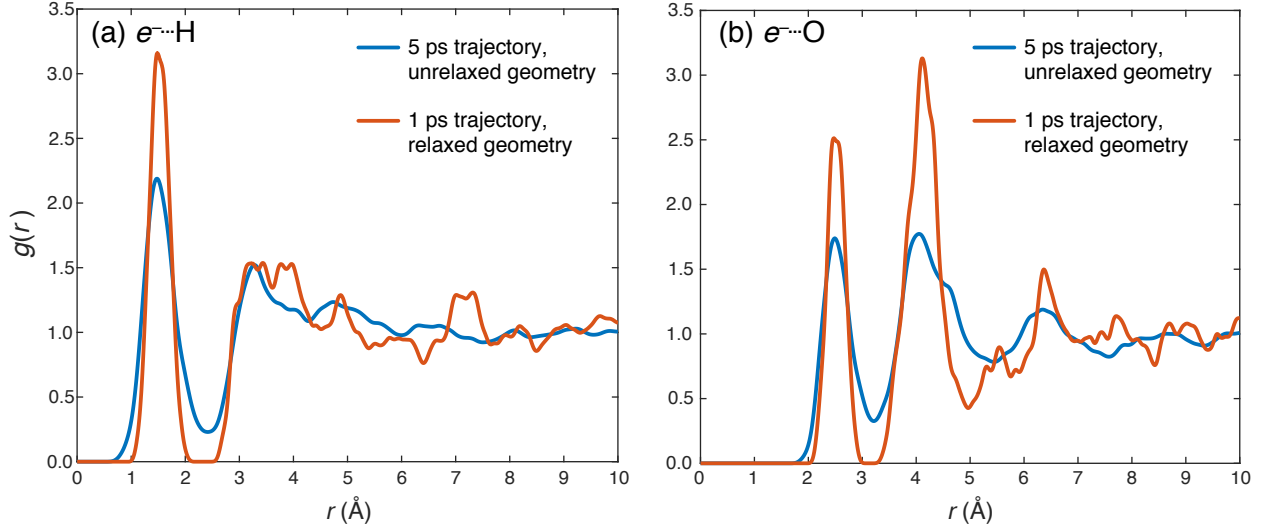


FIG. S2: Radial distribution functions (RDFs) for (a)  $e^- \cdots \text{H}$  and (b)  $e^- \cdots \text{O}$ , where the electron coordinate is the centroid of  $\rho_{\text{spin}}(\mathbf{r})$ . RDFs were computed using either a 5 ps trajectory whose initial geometry as taken from Ref. 5 without alteration, or else a 1 ps trajectory where the structure was first relaxed prior to the MD simulation. (These two trajectories correspond to the energy fluctuations with or without geometry optimization that are shown in Figs. 4 and S1.) The RDFs were smoothed using a Gaussian windowing function whose width is 0.100  $\text{\AA}$  and 0.055  $\text{\AA}$  for  $e^- \cdots \text{O}$  in the shorter and the longer trajectory, respectively. For  $e^- \cdots \text{H}$ , the width is 0.15  $\text{\AA}$  for the shorter trajectory and 0.09  $\text{\AA}$  for the longer one.

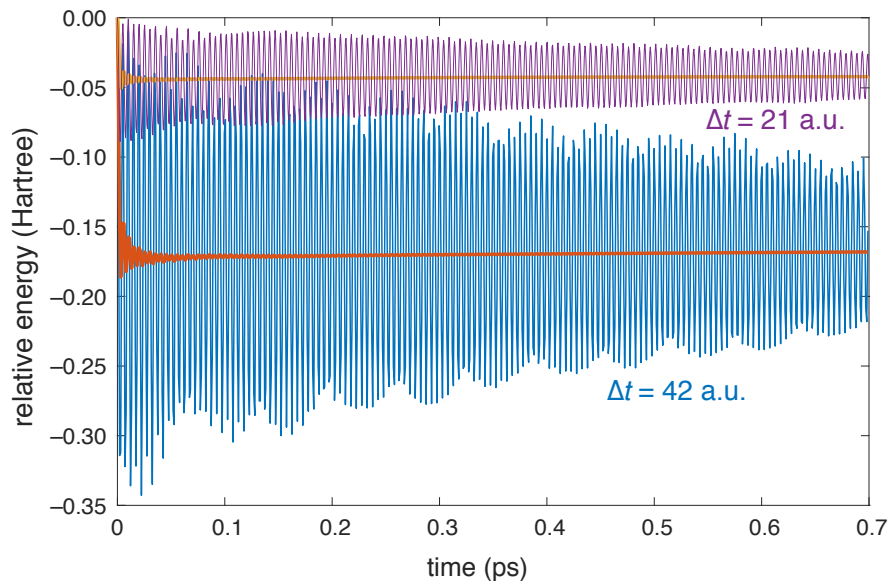


FIG. S3: Energy fluctuations in HF+D3/3-21++G\* simulations of  $e^-(aq)$ , comparing two different time steps. Except for the choice of  $\Delta t$ , the two simulations are run under identical conditions that are consistent with the trajectories reported in the paper. (In particular, the simulations are performed under microcanonical conditions with initial velocities consistent with  $T = 300$  K, in a periodic simulation cell containing a total of 1,024 water molecules, 24 of which are described at a QM level). Energy is plotted relative to its value at  $t = 0$ , and the orange data show the running average of the energy for either simulation.

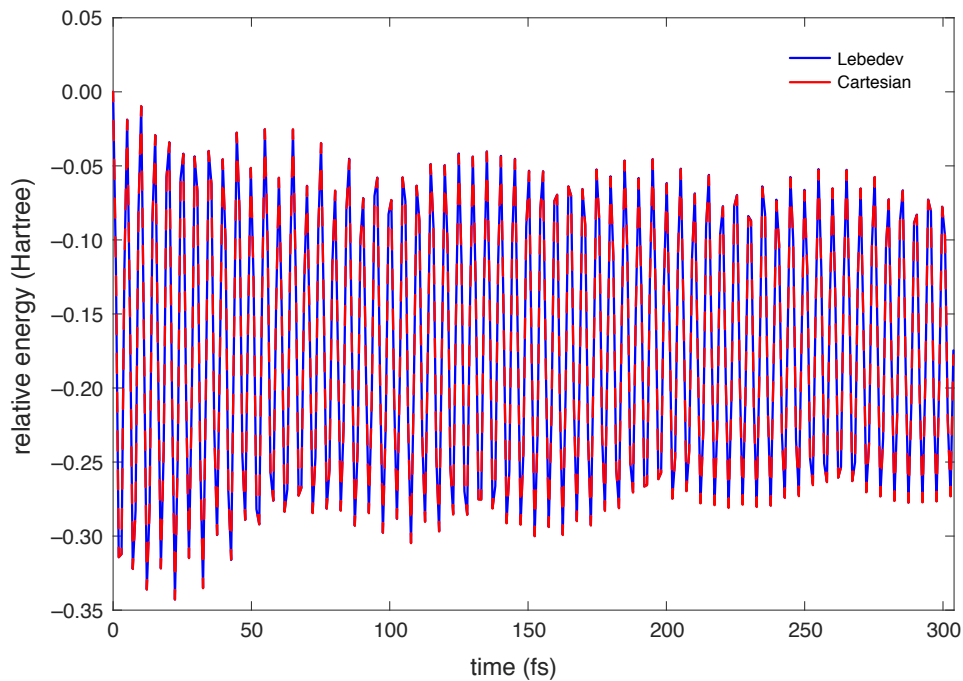


FIG. S4: Energy fluctuations in HF+D3/3-21++G\* simulations of  $e^-$  (aq), using either an atom-centered Lebedev grid (data in blue) or else a uniform Cartesian grid (data in red) to compute the CHELPG charges. Although the choice of grid results in slightly different CHELPG charges, and absolute energies that differ by  $\sim 10^{-4} E_h$ , the effect on the energy fluctuations is indiscernible.

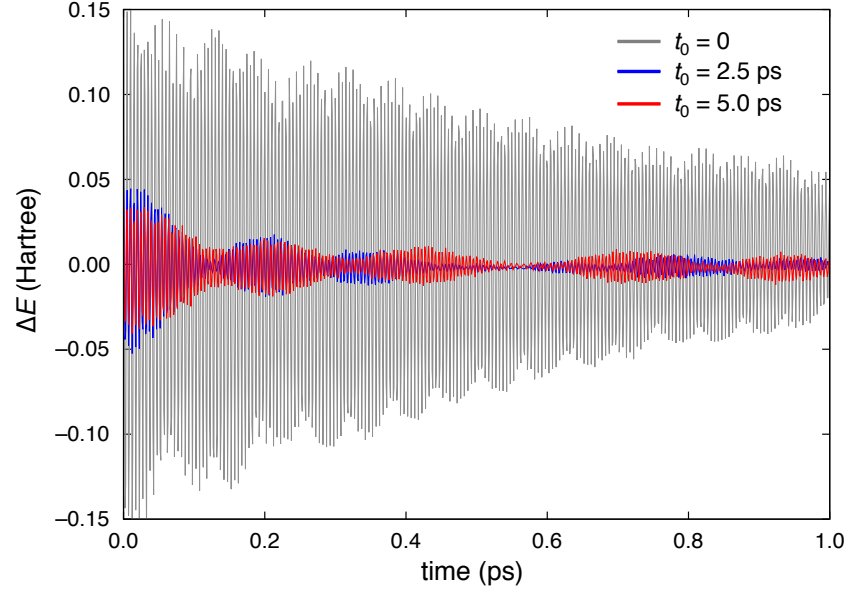


FIG. S5: Energy fluctuations in HF+D3/3-21G\* simulations of *neutral liquid water*, starting from a snapshot of  $e^-(aq)$  (containing a cavity) at time  $t_0$  along the  $e^-(aq)$  trajectory. The force field, simulation cell, and other simulation details are otherwise the same as in the  $e^-(aq)$  simulations. In particular, the simulations are microcanonical (with initial velocities consistent with  $T = 300$  K) and the time step is  $\Delta t = 42$  a.u.



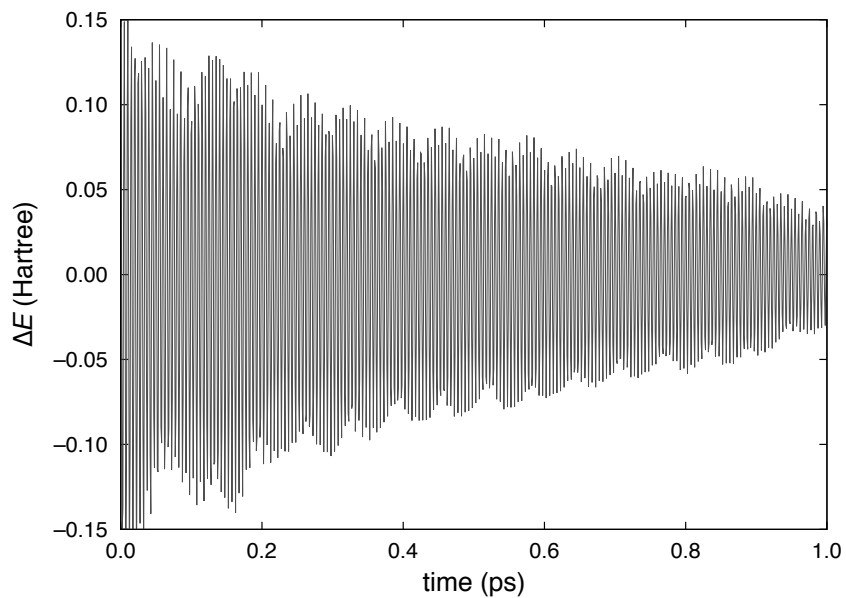


FIG. S6: Energy fluctuations in HF+D3/3-21G\* simulations of *neutral liquid water*, starting from the pre-formed cavity structure used in the  $e^-$ (aq) simulations at  $t = 0$ . Simulation conditions are the same as in Fig. S5 (and thus corresponds to the  $t_0 = 0$  simulation from that figure) except that Mulliken rather than CHELPG charges are used in the QM/MM-Ewald procedure.